https://ieeexplore.ieee.org/abstract/document/7964750
DOI: 10.1109/TITS.2017.2716541

Economic Model Predictive Control of Large-scale Urban Road Networks via Perimeter Control and Regional Route Guidance

Isik Ilber Sirmatel and Nikolas Geroliminis

***Abstract*—Local traffic control schemes fall short of achieving coordination with other parts of the urban road network, whereas a centralized controller based on detailed traffic models would suffer from excessive computational burden. State estimation for detailed traffic models with limited observations and unpredictability of individual driver behavior create additional complications in the applicability of these models for large scale traffic control. These point towards the need for designing network-level controllers building on aggregated traffic models, which have recently attracted attention through the macroscopic fundamental diagram (MFD) of urban traffic. Under some conditions, the MFD provides a unimodal, low-scatter, and demand-insensitive relationship between vehicle accumulation and travel production inside an urban region. In this paper we propose MFD-based economic model predictive control (MPC) schemes to improve mobility in heterogeneously congested large-scale urban road networks. For more realistic simulations of urban networks with route guidance actuation based control, a new model with cyclic behavior prohibition is developed. This paper extends upon earlier works on perimeter control based MPC schemes with MFD modeling by integrating route guidance type actuation, which distributes flows exiting a region over its neighboring regions. Performance of the proposed schemes are evaluated via simulations of congested scenarios with noise in demand estimation and measurement errors. Results show the possibility of substantial improvements in urban network performance, in terms of network delays and traveled distance, even for low levels of driver compliance to route guidance.**

***Index Terms*—Model predictive control (MPC), urban traffic control, perimeter control, route guidance, macroscopic fundamental diagram (MFD).**

I. Introduction

URBAN traffic congestion continues to trouble the cities of modern society and remains a challenging problem. Application of automatic control methods to traffic problems gained increasing interest for ensuring efficient and reliable operation of urban networks (for reviews refer to [1], [2]). Coupling advanced control techniques with complex traffic models requires challenging improvements on both fields. There is considerable literature on methods for controlling a limited area of the urban network, which are usually based on detailed micro- or mesoscopic models and involve control schemes that consider only a small part of the whole urban network, such as a set of signalized intersections. In their locale of operation, these methods provide good performance for undersatured traffic conditions, but they also have important shortcomings: (a) They are inadequate in dealing with congested conditions and heterogeneous distribution/spatiotemporal propagation of congestion (especially when spillbacks occur), (b) there is no coordination between controllers operating in different parts of the network, leading to uncoordinated decisions and potentially conflicts, and ultimately to suffering network performance, (c) they require information on highly detailed traffic states, which might be difficult to measure/estimate. Thus, the need for developing control schemes that can achieve coordination between regions of the network, can handle severely and heterogeneously congested conditions, and rely only on aggregated traffic information that is relatively easy to measure, points to the direction of exploring network-level controllers for large-scale urban road networks. The main idea of network-level aggregated control is to create an additional layer in a hierarchical structure before the local controllers are implemented (see [3]). Improving the overall condition in critical areas of a city can help the aforementioned local schemes to improve the local objectives as disturbances under mild conditions will have less negative effect.

Since the beginning of 1980s many works have focused on modeling and control of urban traffic, which usually consider mesoscopic models with link-level dynamics and controllers using local information. As one of the relatively recent studies, based on the linear-quadratic regulator problem, traffic-responsive urban control (TUC) [4] represents a multivariable feedback regulator approach for network-wide urban traffic control, which has been tested both via simulations and field implementations (see [5]). Although TUC can deal with oversaturated conditions via minimizing and balancing the relative occupancies of network links, it may not be optimal for heterogeneous networks with multiple pockets of congestion. Based on the max-pressure approach, many local control schemes have been proposed for networks of signalized intersections (see [6]–[8]), which involve evaluations at each intersection requiring information exclusively from adjacent links. Although the high level of detail in mesoscopic models is desirable for simulation purposes, the increased complexity results in complications for control. Furthermore, local controllers might not be able to operate properly under heavily congested conditions, as they do not protect the congested regions upstream. Another disadvantage of sophisticated local controllers is that they might require detailed information on traffic states, which are difficult to measure or estimate. The interaction between selfish route choices and the responsive

Isik Ilber Sirmatel and Nikolas Geroliminis are with the School of Architecture, Civil and Environmental Engineering, École Polytechnique Fédérale de Lausanne (EPFL), 1015 Lausanne, Switzerland. {isik.sirmatel,nikolas.geroliminis}@epfl.ch

pressure-driven traffic control policies are discussed in the P0 scheme and its extensions for simple networks (see [9], [10]).

In the recent years, the two layer hierarchical control approach for urban networks appeared as an alternative to the local traffic control methods established in the literature. At the upper layer a network-level controller optimizes network performance via manipulating macroscopic traffic flows through interregional actuation systems (e.g., perimeter control), whereas at the lower layer the local controllers regulate mesoscopic traffic flows through intraregional actuation systems (e.g., signalized intersections). The macroscopic fundamental diagram (MFD) of urban traffic garnered recent interest as a tool for developing aggregated models of urban networks, enabling low complexity modeling of whole cities and efficient network-level control design for the upper layer.

First proposed by [11] and experimentally proven to exist for large-scale urban areas by [12], the MFD enables modeling of an urban region with roughly homogeneous accumulation (i.e., small spatial link density heterogeneity) by providing a unimodal, low-scatter, and demand-insensitive relationship between accumulation and trip completion flow [12]. Although a powerful modeling tool, the MFD has also its challenges, which might undermine its usefulness. Firstly, hysteresis phenomena, which can be observed on the onset or offset of congestion, may adversely affect the shape of the MFD (see [3], [13] for details). Secondly, heterogeneous distribution of accumulation, especially in congested conditions, leads to the loss of a well-defined MFD for the urban region (see [14], [15]). Despite these shortcomings, the MFD substantially reduces the complexity of traffic models, and is thus an efficient modeling tool for expressing aggregated dynamics of urban traffic networks, opening the way for the design of network-level control schemes for the upper layer of the hierarchical approach (integration of clustering techniques are shown to be beneficial with respect to the aforementioned shortcomings, see, e.g., [16], [17]). Thus, in the last decade the MFD attracted interest in the traffic control literature as an aggregated modeling tool for urban networks. MFD-based control schemes have been proposed by many researchers for single-region [18]–[22] and multi-region [3], [23]–[26] urban networks. More detailed literature reviews in MFD-based modeling and control can be found in [27] and [28].

The design of network-level controllers for urban networks with MFD-based modeling requires consideration of the following points: (a) Constraints on the traffic states and control inputs, (b) nonlinear dynamics of the MFD-based network model, (c) possibility of having access to future information (e.g., estimates of the trip demands based on historical data). These points strongly suggest the suitability of model predictive control (MPC), which is an advanced control technique based on real-time repeated optimization, its most important advantage over other control methods being its ability to handle constraints systematically. A computationally efficient method for tackling infinite horizon, constrained optimal control problems (OCPs), MPC provides approximate solutions to such problems via solving a series of finite horizon open-loop OCPs in receding horizon fashion. At each sampling instant, using the current state of the system as initial state, the finite horizon OCP is solved to obtain a sequence of optimal controls, the first of which is applied to the system and the whole procedure is repeated in the next sampling instant. Discussions on important issues of MPC can be found in [29] and an overview of theoretical aspects is given in [30].

Application of MPC to traffic control problems saw increased interest in the ITS literature in the last 15 years: Ramp metering for freeway networks [31]–[33], variable speed limits [34], [35], integration of ramp metering with variable speed limits [36] and with route guidance [37] for freeway networks, signal control for urban networks [38], [39], signal control for mixed urban and freeway networks [40], and control of logistics systems and railways [41], [42].

MPC schemes with MFD-based prediction models for urban networks began to appear only recently in the literature. In the first work on this direction, a nonlinear MPC is proposed for a two-region urban network equipped with perimeter control actuation [43]. For the cooperative control of a mixed transportation network consisting of a freeway and two urban regions, an MPC scheme is developed in [44]. A hybrid MPC is developed in [45] for an urban network equipped with both perimeter control systems and switching signal timing plans. In [3], a model capturing the dynamics of heterogeneity is developed together with a hierarchical control system with MPC on the upper level. The aforementioned works on MFD-based MPC for urban networks do not explore actuation via routing the the drivers. Although there are also some recent attempts on this direction [28], [46], enhancing perimeter control with route guidance actuation still remains unexplored.

In this paper network-level economic MPC schemes integrating perimeter control and regional route guidance are proposed to improve mobility in urban networks. In contrast to standard MPC where the objective function is related to a control goal such as regulation or setpoint tracking, economic MPC involves objective functions that express economically optimal plant operation (e.g., maximizing profits or minimizing time spent). Firstly, a new MFD-based urban network model is developed with cyclic behavior avoidance, i.e., prohibiting vehicles from flowing back and forth between neighboring regions, which is important for simulating urban networks under closed-loop with route guidance based control schemes. Furthermore, the problem of finding the perimeter control and route guidance inputs for a multi-region urban network to minimize total time spent (TTS) is formulated as an economic MPC problem, along with various actuator configurations. The analysis in this work sheds some light to the demand conditions for which coupling of perimeter control and route guidance can prove beneficial. Results indicate that the proposed MPC schemes can significantly decrease network delays and, when route guidance is coupled with perimeter control, even low driver compliance levels are sufficient to improve network performance.

II. Modeling of Large-Scale Urban Networks

A. MFD-based Modeling of a Multi-region Urban Network

We consider an urban network $\mathcal{R}$ with heterogeneous distribution of accumulation, consisting of R homogeneous

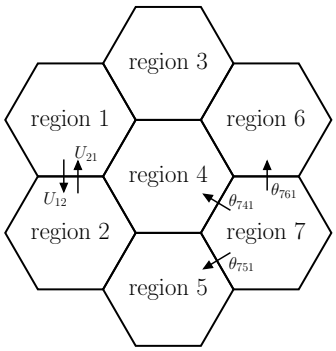

Fig. 1. Schematic of an urban network with 7 regions.

regions, i.e., $\mathcal{R} = \{1, 2, \ldots, R\}$, each with a well-defined outflow MFD, defined via $G_I(N_I(t))$ (veh/s) expressing the trip completion flow (i.e., outflow) at accumulation $N_I(t)$. A network consisting of 7 regions is schematically shown in fig. 1. The exogenous inflow demand generated in region I with destination J is $Q_{IJ}(t)$ (veh/s), whereas $N_{IJ}(t)$ (veh) is the accumulation in region I with destination J, and $N_I(t)$ (veh) the total accumulation in region I, at time t; $I, J \in \mathcal{R}$; $N_I(t) \triangleq \sum_{J\in\mathcal{R}} N_{IJ}(t)$. Between each pair of neighboring regions I and H ($I \in \mathcal{R}$, $H \in \mathcal{N}_I$, where $\mathcal{N}_I$ is the set of regions neighboring region I) there exists perimeter controls $U_{IH}(t)$ and $U_{HI}(t) \in [0, 1]$ that can manipulate the transfer flows. Furthermore, each region is equipped with regional route guidance controls $\theta_{IHJ}(t)$ ($I \in \mathcal{R}$, $H \in \mathcal{N}_I$, $J \in \mathcal{R} \setminus \{I\}$), that can distribute the transfer flows exiting a region over its neighboring regions. Dynamics of an R-region MFDs network are [3], [28]:

$$\dot{N}_{II}(t) = Q_{II}(t) - M_{II}(t) + \sum_{H\in\mathcal{N}_I} U_{HI}(t) M_{HII}(t) \quad (1a)$$

$$\dot{N}_{IJ}(t) = Q_{IJ}(t) - \sum_{H\in\mathcal{N}_I} U_{IH}(t) M_{IHJ}(t) + \sum_{H\in\mathcal{N}_I; H\neq J} U_{HI}(t) M_{HIJ}(t), \quad (1b)$$

for $I, J \in \mathcal{R}$, where $M_{II}(t)$ (veh/s) is the exit (i.e., internal trip completion) flow from region I to destination I:

$$M_{II}(t) = \frac{N_{II}(t)}{N_I(t)} G_I(N_I(t)) \quad (2)$$

and $M_{IHJ}(t)$ (veh/s) is the transfer flow from region I to destination J through the next immediate region H:

$$M_{IHJ}(t) = \theta_{IHJ}(t) \frac{N_{IJ}(t)}{N_I(t)} G_I(N_I(t)), \quad (3)$$

with $M_{HII}(t)$ and $M_{HIJ}(t)$ defined similarly, expressing the transfer flows from H through I with destinations I and J, respectively. It is assumed that trips inside a region have similar lengths (i.e., the distance traveled per vehicle inside a region does not depend on the origin and destination of the trip). Simulation and empirical results [12] suggest that the MFD can be approximated by an asymmetric unimodal curve skewed to the right (i.e., the critical accumulation N_I^{cr}, which maximizes $G_I(N_I(t))$, is less than half of the jam accumulation N_I^{jam}, which puts the region in gridlock). Thus, $G_I(N_I(t))$ can be expressed with a third-order polynomial in the variable $N_I(t)$, i.e., $G_I(N_I(t)) = A_I N_I^3(t) + B_I N_I^2(t) + C_I N_I(t)$, where A_I, B_I, and C_I are estimated parameters.

Transfer flows are influenced by the boundary capacity between regions I and H, as high accumulation in region H might restrict the reception of inflows from the boundary, which can be formalized through the following equation expressing capacity-restricted transfer flow $\hat{M}_{IHJ}(t)$ [3], [28]:

$$\hat{M}_{IHJ}(t) = \min\left(M_{IHJ}(t), C_{IH}(N_H(t)) \frac{M_{IHJ}(t)}{\sum_{K\in\mathcal{R}} M_{IHK}(t)} \right) \quad (4)$$

where $C_{IH}(N_H(t))$ (veh/s) is the boundary capacity between regions I and H that depends on N_H as follows [3]:

$$C_{IH}(N_H) = \begin{cases} C_{IH}^{\max} & \text{if } 0 \le N_H < \alpha \cdot N_{H,\text{jam}} \\ \frac{C_{IH}^{\max}}{1-\alpha}\left(1 - \frac{N_H}{N_H^{\text{jam}}}\right) & \text{if } \alpha \cdot N_H^{\text{jam}} \le N_H \le N_H^{\text{jam}}, \end{cases} \quad (5)$$

where $C_{IH}^{\max}$ (veh/s) is the maximum boundary capacity, N_H^{jam} (veh) is the jam accumulation of the receiving region H, whereas $\alpha \cdot N_H^{\text{jam}}$ (with $0 < \alpha < 1$) specifies the point where $C_{IH}(N_H)$ starts decreasing with increasing accumulation.

The boundary capacity constraint can be omitted in the prediction model of MPC for computational advantage. The physical reasoning of this omission is that (i) the boundary capacity decreases for accumulations much larger than the critical accumulation, and (ii) the controller will not allow the regions to have accumulations close to gridlock [44]. The effect of tightening boundary capacity is studied in section IV-F.

The assumption of a low-scatter regional outflow MFD is based on the equivalent assumption of a time-invariant regional trip length. While an adequate model for control design with simplified system dynamics without delays (i.e., it considers outflows equal to the ratio of production over constant trip length), and although there are empirical verifications about its validity via aggregated data (e.g., [12]), the MFD should not be considered as a universal law. For example, strong fluctuations in the demand that create fast evolving transients can influence the trip length distribution in a region at a specific time, potentially causing the ratio of production over trip length approximation of outflow to have inaccuracies. While we consider this a valid assumption for a range of cases, further research would be useful to study under what conditions more complex dynamics (with delays) are required (see, e.g., some analysis in [47]), which is a research priority.

B. Cyclic Behavior Prohibiting Urban Network Model

The urban network model (1) has no memory of the region the vehicles were previously, thus does not prohibit vehicles from flowing back and forth between neighboring regions (i.e., it permits cyclic behavior). While this memoryless choice of routes is not crucial when only perimeter control actuation is applied, it is physically important for route guidance based schemes, where the controller may try to emulate perimeter control actuation via cyclic routes. We also need to be able to compare travel times and trip lengths for inflow demands

$Q_{IJ}(t)$ and for various control strategies and driver compliance levels. Thus, instead of N_{IJ} and M_{IHJ} we have to introduce more detailed states. With N_{OGIJ} and M_{OGIHJ} denoting the accumulation and flow, respectively, with origin O, previous region G, current region I, destination region J, and immediate next region H, the dynamics keeping memory of origin and previous regions can be written as:

$$\dot{N}_{IIII}(t) = Q_{II}(t) - M_{IIIII}(t),\ \forall I \in \mathcal{R}, \tag{6a}$$

$$\dot{N}_{IIIJ}(t) = Q_{IJ}(t) - \sum_{H\in\mathcal{N}_I} U_{IH}(t) M_{IIIHJ}(t), \quad \forall I, J \in \mathcal{R},\ J \neq I, \tag{6b}$$

$$\dot{N}_{OGII}(t) = \sum_{F\in\mathcal{N}_G^*\setminus\{I\}} U_{GI}(t) M_{OFGII}(t) - M_{OGIII}(t), \quad \forall O, G, I \in \mathcal{R},\ G \in \mathcal{N}_I,\ O \neq I, \tag{6c}$$

$$\dot{N}_{OGIJ}(t) = \sum_{F\in\mathcal{N}_G^*\setminus\{I,J\}} U_{GI}(t) M_{OFGIJ}(t) - \sum_{H\in\mathcal{N}_I\setminus\{O,G\}} U_{IH}(t) M_{OGIHJ}(t), \quad \forall O, G, I, J \in \mathcal{R},\ G \in \mathcal{N}_I,\ O \neq I,\ O \neq J,\ G \neq J,\ J \neq I, \tag{6d}$$

where $\mathcal{N}_G^*$ is the set containing the neighboring regions of G and region G itself. Note that if the last two indices of a flow term are identical, then this denotes an exit flow (as next and final region are the same); it denotes a transfer flow otherwise. Note that in (6a) there are no control inputs as flows are internal and uncontrolled. Note also that in (6c)–(6d) the positive terms of the right hand side are controlled transfer flows from the neighboring regions to the current region. The exit and transfer flow terms can be calculated as follows:

$$M_{OGIHJ}(t) = \theta_{OGIHJ}(t) \frac{N_{OGIJ}(t)}{N_I(t)} G_I(N_I(t)), \tag{7}$$

where θ_{OGIHJ} denotes the fraction of flows in an identical way with the flow terms, having the same 5 indices.

Using (6) as the simulation model (i.e., the *plant* representing reality) with MPC controllers having (1) as the prediction model requires the transfer of variables between the two models as follows:

$$\sum_{O\in\mathcal{R}\setminus\{J\}} \sum_{G\in\mathcal{R}\setminus\{J\}} N_{OGIJ}(t) = N_{IJ}(t),\ \forall I, J \in \mathcal{R} \tag{8}$$

for the accumulations states and

$$\theta_{OGIHJ}(t) = \begin{cases} \theta_{IHJ}(t) & \text{if } H \neq G, \\ 0 & \text{otherwise} \end{cases} \tag{9}$$
$$\forall O, G, I, J \in \mathcal{R},\ G \in \mathcal{N}_I,\ H \in \mathcal{N}_I \setminus \{O\},\ O \neq I,\ O \neq J,\ G \neq J,\ J \neq I$$

for the fraction of flows, where cycle-inducing θ_{OGIHJ} terms (i.e., those with $H = G$) are forced to be 0. Owing to this, the model (6) can prohibit cycles of length 2, and is thus a more realistic representation of urban network dynamics. For prohibiting longer cycles, (6) should be extended with longer route memory, but this is not considered in this work since cycles longer than two are assumed to be negligible.

III. Optimal Control of Urban Networks via Perimeter Control and Regional Route Guidance

A. Model Predictive Control Problem Formulation

We formulate the problem of finding the U_{IH} and θ_{IHJ} values that minimize TTS (for a finite horizon) as the following discrete time economic nonlinear MPC problem:

$$\begin{aligned}
\underset{U,\,\theta}{\text{minimize}} \quad & T_c \cdot \sum_{k=0}^{N_p-1} \|N(k)\|_1 \\
\text{subject to} \quad & N(0) = \hat{N}(t_c) \\
& \left|U(0) - \hat{U}(t_c - 1)\right| \leq \Delta_U \\
& \left|\theta(0) - \hat{\theta}(t_c - 1)\right| \leq \Delta_\theta \\
& \text{for } k = 0, \ldots, N_p - 1: \\
& \quad N(k+1) = f(N(k), Q(k), U(k), \theta(k)) \\
& \quad 0 \leq \sum_{j\in\mathcal{R}} N_{IJ}(k) \leq N_I^{\text{jam}},\ \forall I \in \mathcal{R} \\
& \quad U_{\min} \leq U_{IH}(k) \leq U_{\max},\ \forall I \in \mathcal{R}, H \in \mathcal{N}_I \\
& \quad 0 \leq \theta_{IHJ}(k) \leq 1,\ \forall I, J \in \mathcal{R}, I \neq J, H \in \mathcal{N}_I \\
& \quad \sum_{H\in\mathcal{N}_I} \theta_{IHJ}(k) = 1,\ \forall I, J \in \mathcal{R}, I \neq J \\
& \quad \text{if } k \geq N_c: \\
& \quad\quad U(k) = U(k-1) \\
& \quad\quad \theta(k) = \theta(k-1),
\end{aligned} \tag{10}$$

where T_c is the control sampling time, $N(k)$, $Q(k)$, $U(k)$, and $\theta(k)$ are vectors containing all $N_{IJ}(k)$, $Q_{IJ}(k)$, $U_{IH}(k)$, and $\theta_{IHJ}(k)$ terms, respectively, with k being the control interval counter, f is the time discretized version of eq. (1)–(3), t_c is the current control time step and $\hat{N}(t_c)$ is the measurement taken at t_c, $\hat{U}(t_c - 1)$ and $\hat{\theta}(t_c - 1)$ are the control inputs applied to the plant previously, N_p and N_c are the prediction and control horizons, whereas Δ_U and Δ_θ are the rate limits on perimeter control and route guidance inputs, respectively.

The problem (10) is a nonconvex nonlinear program (NLP), which can be solved efficiently via, e.g., sequential quadratic programming (SQP) or interior point solvers.

We propose three MPC schemes: (i) perimeter control MPC (PC) has U_{IH} as control input, while drivers are free to choose their own routes (i.e., θ_{IHJ}), which are assumed fixed to their measured value, at t_c, for the prediction horizon. (ii) For route guidance MPC (RG) θ_{IHJ} is the control input, while U_{IH} is fixed to $U_{\max}$. (iii) Perimeter control and route guidance MPC (PCRG) has access to both actuators. While $\theta_{IHJ}(t_c)$ is difficult to estimate with fixed location sensors, use of mobile sensors with advanced estimation techniques provide strong potential in this direction (see, e.g., [48]).

Performance metrics for evaluating the MPC schemes are TTS and *total traveled distance* (TTD):

$$\text{TTS} = T_s \cdot \sum_{t=1}^{T_{\text{exp}}} \sum_{I\in\mathcal{R}} N_I(t),$$

$$\text{TTD} = T_s \cdot \sum_{t=1}^{T_{\text{exp}}} \sum_{I\in\mathcal{R}} L_I \cdot \left(M_{II}(t) + \sum_{H\in\mathcal{N}_I} \sum_{J\in\mathcal{R}\setminus I} \bar{M}_{IHJ}(t) \right),$$

where the flow $\bar{M}_{IHJ}(t)$ (veh/s) is defined as $\bar{M}_{IHJ}(t) = U_{IH}(t)\theta_{IHJ}(t)M_{IJ}(t)$. It is important to look at both performance metrics, as route guidance might enforce some drivers to take significantly longer routes for the system benefit. Such a result would be difficult to be acceptable in practice as drivers would follow the proposed routes only if their individual travel time is not significantly worse.

For a single-region city governed by an outflow MFD, minimizing TTS will result in maximizing outflow (which is equivalent to maximizing TTD), as the objective is to let vehicles finish their trips as soon as possible. Thus, as proven in [18], the best strategy is to keep the region at its critical accumulation if the delays of vehicles waiting outside the network (i.e., the virtual queues) are considered.

For a multi-region city (as is the case in the paper), however, it might be impossible to keep all regions under or at critical accumulation. Then, control via tracking regional accumulation setpoints is difficult, as it is not straightforward to find those setpoints that minimize TTS (since these might be time-varying and depend on the demand pattern). Maximizing TTD, on the other hand, might create very long routes for some vehicles especially under uncongested conditions due to detouring, which would decrease network outflow.

B. Controller Tuning and Computational Efficiency

MPC performance is strongly influenced by the prediction horizon N_p. Computational effort is affected also by the chosen direct method and NLP solver (see [49] for details). To study the relations between all of the above, a series of simulation experiments (based on the congested scenario in section IV-B) is conducted with varying values of N_p (with N_c fixed to 2 and a control sampling time of $T_c = 240$ s) and various direct methods (see [50] for details). Direct multiple shooting (DMS, [51]) and direct collocation (DC) (solved with the solver IPOPT [52]) results for all three MPC schemes[1] are included together with direct single shooting (DSS) (solved with an SQP solver) for PC. Using SQP for DMS and DC is computationally disadvantageous, since SQP favors small and dense NLPs (such as those arising from DSS), while DMS and DC yield large and sparse NLPs (which are amenable to efficient solutions via e.g. IPOPT). The results, given in fig. 2, show the TTS performance and the average CPU times, which indicate that: (a) TTS performance is fairly insensitive to the choice of N_p for $N_p \geq 7$, (b) DSS is favorable for PC, whereas DC is favorable for RG and PCRG, (c) even for short horizons PCRG is able to yield high improvements.

IV. Case Studies

A. Network Description and Simulation Setup

All simulations are conducted on a 7 region urban network (see fig. 1), with the simulation model given in (6) for representing the reality. A unit MFD is considered with the parameters $\bar{A} = 4.133 \cdot 10^{-11}$, $\bar{B} = -8.282 \cdot 10^{-7}$, $\bar{C} = 0.0042$,

[1]Implementation is done via the CasADi toolbox [53] in MATLAB 8.5.0 (R2015a), on a 64-bit Windows PC with 3.6-GHz Intel Core i7 processor and 16-GB RAM.

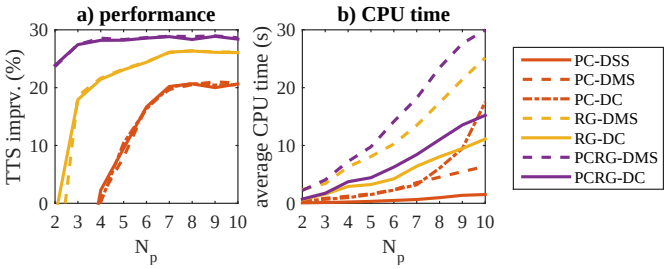

Fig. 2. (a) Percent improvement in TTS over NC and (b) average CPU times for the MPC schemes with various direct methods as a function of N_p.

jam accumulation $\bar{N}^{\text{jam}} = 10^4$ (veh), critical accumulation $\bar{N}^{\text{cr}} = 3.4 \cdot 10^3$ (veh), maximum outflow $G(\bar{N}^{\text{cr}}) = 6.3$ (veh/s), with an average trip length of $\bar{L} = 3600$ m, which are consistent with the MFD observed in a part of downtown Yokohama (see [12]). Each region is assumed to have a different MFD that is a (within $\pm 10\%$) scaled version of the unit MFD. Boundary capacity effect is included, with values $\bar{C}_{IH}^{\max} = 3.2$ veh/s and $\bar{\alpha} = 0.64$ for the unit MFD.

Based on the results in section III-B, the prediction and control horizons are chosen as $N_p = 7$ and $N_c = 2$ for the MPC schemes. Simulation sampling time is 30 s while the length of the simulation experiment is $T_{\text{exp}} = 240$ (in number of simulation steps), giving an effective length of 120 minutes. Bounds of U_{IH} are $U_{\min} = 0.1$ and $U_{\max} = 0.9$, whereas the rate limits are $\Delta_U = 0.2$ and $\Delta_\theta = 0.1$, to reflect the fact that it is more difficult to cause abrupt changes in routing.

For capturing the effect of measurement noise in accumulation states (as accumulations have to be measured from fixed and mobile sensors, which invariably have noise), we add random noise terms with normal distribution:

$$\tilde{N}_{IJ}(t) = N_{IJ}(t) + N_{IJ}(t) \cdot \mathcal{N}(0, \sigma^2_{N_{IJ}}), \ \forall I, J \in \mathcal{R}, \quad (11)$$

where the noise has zero mean and its variance is chosen as $\sigma^2_{N_{IJ}} = 0.25$ in the simulations. Demand uncertainty is also considered, with the MPC having access to average demand profiles, while the actual inflow demands have random noise:

$$\tilde{Q}_{IJ}(t) = Q_{IJ}(t) + Q_{IJ}(t) \cdot \mathcal{N}(0, \sigma^2_{Q_{IJ}}), \ \forall I, J \in \mathcal{R}, \quad (12)$$

with the variance chosen as $\sigma^2_{Q_{IJ}} = 0.25$ in the simulations, representing presence of large noise.

The MPC controllers are compared with a *no control* (NC) case, in which U_{IH} are fixed to $U_{\max}$, while drivers are free to choose their routes. In simulations this is captured by calculating θ_{IHJ} by a logit model (see [54]) using the current travel times from I to destination J through a predefined finite number of shortest sequences of regions connecting the two, calculated with Dijkstra's algorithm for K-shortest paths ($K = 3$ for this paper). As drivers adapt to traffic conditions in real time, the θ_{IHJ} values are updated at each control time step. The logit model relaxes the assumption that drivers always choose the physical shortest path. Simulations using logit model thus tend to be more realistic as drivers rarely have perfect information and do not always behave as rational actors. Parameters of the logit model can be adjusted

to reflect the amount of information available to drivers or their sensitivity to travel time differences between routes.

An interesting point to investigate is about deciding what the preferred actuation scheme is (i.e., PC, RG, or PCRG) under different demand conditions, given that there is a nonnegligible installation cost. While in principle the regions of the city that attract most of the trips should operate at the critical accumulation that maximizes flow (e.g., [18] proves this for single region systems), this might not be the case for multiple regions with competing objectives. Our objective is also to investigate the attractivity of the regions of a city with respect to (i) destinations and (ii) crossing zones. While point (i) is clear, with respect to point (ii) a region might attract a lot of trips simply because many shortest paths are passing from this region (even if destinations are elsewhere). Thus, two simulation parameters are defined to construct various scenarios: (a) The ratio of demands with destination region 4 (i.e., city center) to demands from periphery to periphery, denoted by ρ and (b) driver compliance level, denoted by γ. The ratio ρ, expressing the relative intensity of the inflow demands towards city center, is defined as follows:

$$\rho = \frac{\sum_{t=1}^{T_{\text{exp}}} \sum_{I \in \mathcal{R}} Q_{I4}(t)}{\sum_{t=1}^{T_{\text{exp}}} \sum_{I \in \mathcal{R}\setminus\{4\}} \sum_{J \in \mathcal{R}\setminus\{4\}} Q_{IJ}(t)}, \qquad (13)$$

whereas the driver compliance level γ (also defined as a constant for a single simulation experiment) indicates the percentage of drivers following the route guidance recommendations of the traffic control scheme (i.e., either RG and PCRG), which is used in obtaining the route guidance command θ_{IHJ} value for the control step t_c as follows:

$$\theta^{\text{real}}_{IHJ}(t_c) = \gamma \theta^{\text{MPC}}_{IHJ}(t_c) + (1-\gamma)\theta^{\text{logit}}_{IHJ}(t_c), \qquad (14)$$

where $\theta^{\text{real}}_{IHJ}(t_c)$ is the realized route guidance command (i.e., the value used in simulation), whereas $\theta^{\text{MPC}}_{IHJ}(t_c)$ and $\theta^{\text{logit}}_{IHJ}(t_c)$ are the outputs of the MPC and the logit model, respectively.

B. Control Performance under Congested Conditions

Let us describe the base case scenario: The network is uncongested at the beginning, but faces increased inflow demands as time progresses. The driver compliance level γ is 100% and ratio of demands ρ is equal to 0, meaning no trips have city center as destination–nevertheless this is an important region of attraction as many trips prefer to cross the center due to short distance. The results are given in fig. 3, where the evolution of regional accumulations (fig. 3a to 3d) are shown alongside graphs of time spent in network (fig. 3e), cumulative traveled distance (fig. 3f), outflow of city center (i.e., region 4) (fig. 3g), and the noisy inflow demands $\tilde{Q}_{IJ}(t)$ (fig. 3h), all as a function of simulation time, for the no control (NC) case and the three MPC schemes (please refer to the legends in fig. 3 for descriptions of each figure). A summary of the results is given in table I, which shows the two performance metrics about time and distance (i.e., TTS and TTD), improvement over the NC case for TTS, increase in TTD over the theoretically possible minimum TTD (which is calculated by considering that all vehicles are able to take the physical shortest path to their destinations under free flow conditions, and is equal to $3.87 \cdot 10^8$ veh·m), and the CPU times for the MPC schemes. The results indicate that all MPC schemes are capable of improving mobility in the urban network, as they have decreased values of both the TTS and TTD metrics, in comparison to the NC case. Noting that control sampling time T_c is chosen as 240 s, the CPU time results given in table I suggest that the schemes are computationally tractable, as their CPU times are negligible in comparison to T_c.

TABLE I
PERFORMANCE EVALUATION FOR CONGESTED SCENARIO

Control scheme	TTS ($\times 10^7$ veh·s)	TTS decrease over NC (%)	TTD ($\times 10^8$ veh·m)	TTD increase over theo. min. (%)	Avg. CPU time (s)	Max. CPU time (s)
NC	9.50	–	4.81	25	–	–
PC	7.58	20	4.60	19	0.66	1.59
RG	7.02	26	4.47	16	6.43	8.22
PCRG	6.76	29	4.35	13	8.45	10.18

PCRG is superior in distributing the vehicle flows efficiently over the whole network, which translates to efficient usage of the network capacity, leading to less congestion and also decreased values of TTS. This is clearly seen in the regional accumulation plots (b)–(d) in fig. 3, where PCRG can suppress congestion evenly in all regions. Note also that for all three strategies not all regions are able to operate below the critical value of accumulation, so even the best control scheme still experiences some congestion for some regions, notably for smaller durations. This highlights the importance of using prediction and aggregated future O-D information via MPC. For example, PI type controllers without demand information (see [19], [24], [55]) are successful when all regions can operate close to their critical accumulations. But if this is not possible due to high demand, aggregated O-D information is expected to further improve network performance.

The NC case cannot avoid severe congestion close to gridlock, leading to drastic decrease in outflow for the city center (as seen in fig. 3g) and thus inefficient use of the city center capacity for transferring flows from periphery to periphery. This is crucial for both TTS and TTD metrics, since routes through the city center are generally the physical shortest paths connecting two opposing peripheral regions. The MPC schemes, on the other hand, make efficient use of the city center as seen in the city center outflow (i.e., $G_4(N_4(t))$) plot in fig. 3g, which shows their success in keeping the city center close to critical accumulation N_4^{cr} until network starts to unload. It is interesting that city center remains severely congested even if drivers are adaptive and update their routes based on travel time information (i.e., the NC case), which is not the case when control is applied.

Route guidance based schemes can improve both TTS and TTD metrics compared to the PC scheme due to their authority over routing, increasing the percentage of drivers using the physical shortest path. Thus, vehicles spend less time and travel for shorter distances before exiting the network. The percentage of drivers that are momentarily using the physical shortest path to their destinations is given in fig. 4 for NC

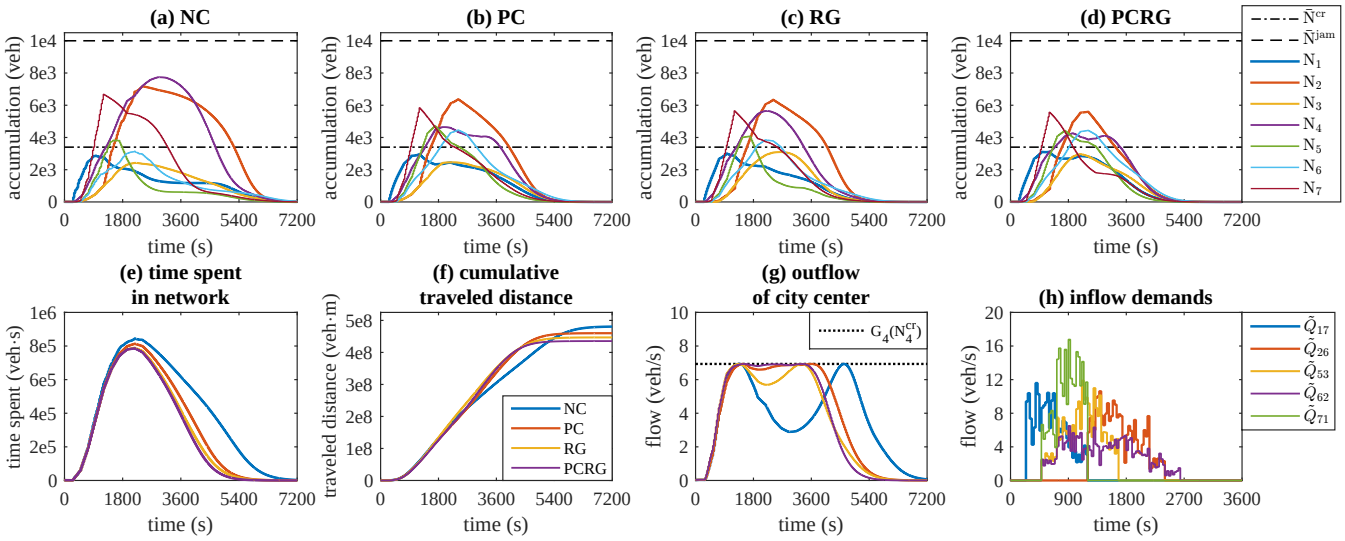

Fig. 3. Results of the congested scenario for the no control (NC) case and the three MPC schemes. Regional accumulations for (a) NC, (b) PC, (c) RG, (d) PCRG. Comparison of the four cases for (e) time spent in network, (f) standard deviation of regional accumulations, (g) outflow of city center. (h) Noisy inflow demand profiles, expressing demands for trips between 5 origin-destination region pairs.

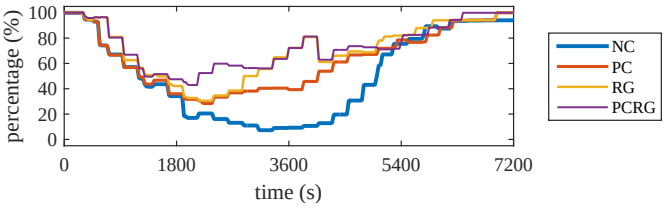

Fig. 4. Usage of physical shortest path for the congested scenario.

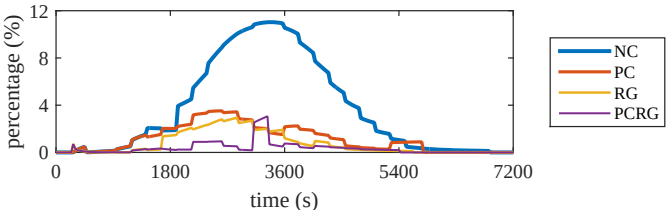

Fig. 5. Ratio of cyclic to total flows for NC and the three MPC schemes.

and the three MPC schemes. This result shows that route guidance based schemes succeed in making more drivers use the physical shortest path, explaining the improvement in TTD. The fact that regional route guidance (which tries to develop conditions close to system optimum) might create worse travel times for some users is analyzed later in the paper.

C. Effect of Cyclic Behavior Prohibition

To examine the effect of absence of cyclic behavior prohibition in the proposed model, given in section II-B, a series of simulation experiments are conducted based on the scenario in section IV-B. The model formulation is changed via relaxing the condition $H \neq G$ in eq. (9) so as to allow cyclic flows. To summarize the presence of cyclic behavior, the percentage of vehicle flows that are returning to the region they came from among the total vehicle flows is considered:

$$\frac{\sum_{O\in\mathcal{R}}\sum_{K\in\mathcal{R}\setminus G}\sum_{G\in\mathcal{R}\setminus K}\sum_{K\in\mathcal{R}\setminus G}\sum_{J\in\mathcal{R}}\bar{M}_{OKGKJ}(t)}{\sum_{O\in\mathcal{R}}\sum_{G\in\mathcal{R}}\sum_{I in\mathcal{R}}\sum_{H\in\mathcal{R}}\sum_{J\in\mathcal{R}}\bar{M}_{OGIHJ}(t)},$$

where the vehicle flow $\bar{M}_{OGIHJ}(t)$ is defined as follows

$$\bar{M}_{OGIHJ}(t) = U_{IH}(t)\theta_{OGIHJ}(t)M_{OGIJ}(t).$$

The results are given in fig. 5, showing this percentage as a function of simulation time. There are substantial cyclic flows occurring in the simulation, which can be avoided with the use of the proposed model, supporting the use of such a model with more detailed states to represent the plant.

D. Driver Compliance and Demand Ratio ρ Analysis

In an ideal case with route guidance actuation, all drivers would follow θ_{IHJ} exactly, but this may not be the case in reality as some drivers might prefer choosing their own routes. To analyze how driver compliance affects route guidance performance, a series of simulations with four different values of ρ are conducted by varying compliance level γ from 0% to 100%, which are summarized in fig. 6. Interestingly, the results differ with varying ratio of demand that has the city center as a destination: For low values of ρ, i.e., for the case with most of the trips from periphery to periphery, these results show that: (a) PC is not very successful in decreasing TTS, while RG performs well for high compliance; thus, PC is not very appropriate when destinations are distributed all over the city and the city center is used mainly for crossing trips, (b) there is no difference between RG and PCRG schemes. For high ρ values, on the other hand, the results indicate: (a) Increasing γ, especially for RG, yields in larger performance improvements, (b) there are substantial differences between RG and PCRG. Specifically, for the case with $\rho = 0.35$, RG cannot prevent gridlock for γ lower than 0.8, whereas PCRG is able to prevent it for γ higher than 0.5, showcasing the superiority

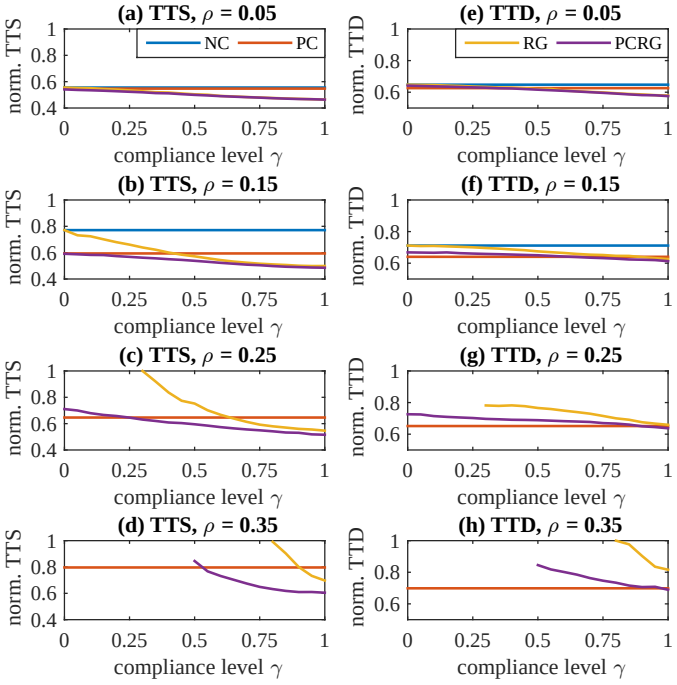

Fig. 6. Performance comparison of the NC case and the three MPC schemes, for different values of ρ, as a function of driver compliance level γ: (a)–(d) normalized TTS, (e)–(h) normalized TTD.

of PCRG over RG in improving network performance even in difficult demand conditions (i.e., high ρ) and low compliance. Besides the performance improvement aspect of these results, an intuition with respect to field implementations can be developed: When a small number of destinations is within the city center, a route guidance system would be sufficient and perimeter control is not necessary. This might happen if the city center has high quality public transport and expensive parking, discouraging people to travel by car in the center. If the number of destinations in the center is higher, then perimeter control is beneficial as it can prevent the center from overcrowding even for low levels of compliance. Furthermore, while RG and PCRG have similar performance for high compliance (with the exception of many city center trips, i.e., for $\rho = 0.35$), the difference is highly pronounced for lower compliance levels. This highlights the importance of coupling PC with RG for realistic implementations, as γ might not be very high due to issues of acceptance by the whole population of drivers and lack of smart technologies in some cars.

E. A More Detailed Consideration of Travel Time Benefits

Control via route guidance may cause some drivers to experience longer travel times compared to cases with no route guidance, leading to lower compliance and finally in less efficient schemes due to low user acceptance. To examine the travel time benefit of drivers under the RG and PCRG schemes, compared to the PC scheme, a series of simulation experiments are conducted with four different values of ρ and γ. For each MPC scheme, the travel times of each group of users with a certain regional O-D are estimated as a function of time based on the horizontal distance between the cumulative departure-

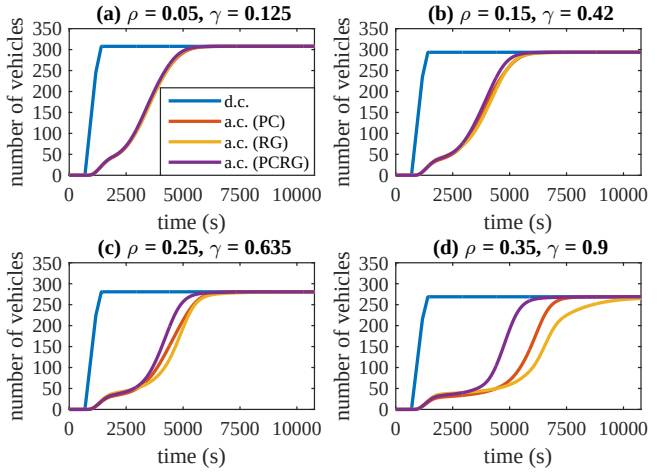

Fig. 7. Departure curve (d.c.) and arrival curves (a.c.) for the three MPC schemes, for the O-D pair 1–7.

arrival curves. Figure 7 provides the cumulative curves for the three schemes (departure curve is the same, as each scheme is tested with the same demand) for O-D pair 1–7. While for small ρ and in the beginning of each case the three schemes are very similar, when a higher number of trips has the center as destination (i.e., for high values of ρ), PCRG performs better than PC and RG. Based on these estimations the distribution of travel time benefits of RG and PCRG are compared to PC, which does not have any ability to control individual O-D movements. The distributions, given in fig. 8, consist of all O-D pairs and times, and are for 4 different values of ρ, each case having a constant value of γ (for each case separately, this corresponds to the γ value for which PC and RG have the same TTS performance). The distributions are skewed and contain both positive and negative values indicating the influence of the schemes for different users. These results indicate the superiority of PCRG over RG, as it keeps almost all drivers better off in terms of experienced travel times: In all cases, roughly 90% of drivers benefit from PCRG, and in general only 2-3% experience travel times extended longer than 5 minutes, suggesting substantial potential for practice.

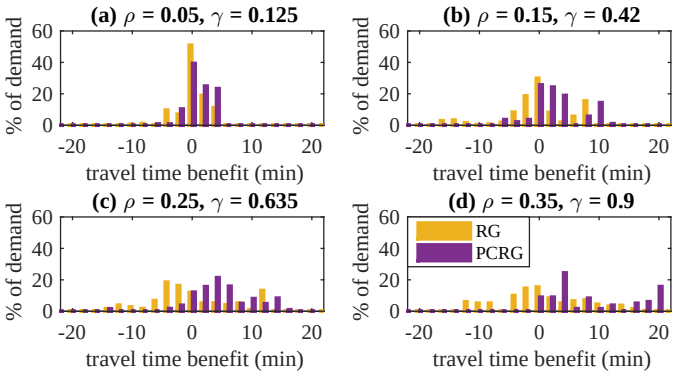

Fig. 8. Travel time benefit of drivers in RG and PCRG schemes with respect to PC scheme, for ρ values of 0.05, 0.15, 0.25, and 0.35, for a constant γ separately for each ρ value.

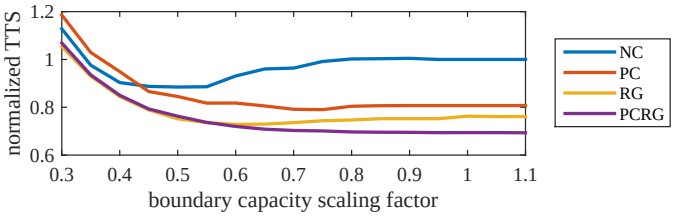

Fig. 9. Sensitivity of TTS performance to changes in boundary capacity.

F. Sensitivity to Changes in Boundary Capacity

To study the effect of the boundary capacity, a series of simulation experiments are conducted via scaling the parameters $C_{IH}^{\max}$ (maximum capacity) and α (specifies the accumulation for which the capacity starts decreasing) used for the congested scenario in IV-B by factors varying from 0.3 to 1.1 (capacities are non-binding above 1.1). The results, given in fig. 9, show that the MPC schemes are fairly insensitive to changes in boundary capacity for factors larger than 0.6, supporting the initial conjecture that boundary capacity can be ignored in the MPC prediction model. Interestingly, boundary capacity seems to provide benefits similar to perimeter control for those cases without actual perimeter control, as seen from the decreased TTS for factors around 0.5 for NC and 0.6 for RG.

V. Conclusion

The paper contributes in two aspects: (a) In the traffic modeling side a novel cyclic behavior prohibiting dynamic urban network model is proposed, with the potential of yielding more realistic simulation results compared to current MFD-based urban network models in the literature, (b) in the control design aspect, integrating perimeter control and route guidance type actuators, economic nonlinear MPC schemes are developed for improving mobility in urban networks. Simulation studies show the potential for substantial improvement in mobility through the use of route guidance, in comparison to control via perimeter control only. A further observation is that since route guidance actuation cannot restrict flows, unlike perimeter control, it is unable to protect urban regions from severe congestion especially for cases with imperfect driver compliance. Highest performance is obtained by using both types of actuators.

Future research could include (a) comparison of the proposed schemes with other approaches (e.g., feedback perimeter control [24], [25]), (b) more detailed simulation experiments with micro- or mesoscopic methods, (c) design of route guidance based control schemes for mixed urban-freeway networks, (d) field implementation. A field test is under preparation for estimation of θ_{IHJ} values through cellphone data in a Swiss city and integration of this information in a PC scheme (with possibility of extension to PCRG cases).

References

[1] M. Papageorgiou, C. Diakaki, V. Dinopoulou, A. Kotsialos, and Y. Wang, "Review of road traffic control strategies," *Proceedings of the IEEE*, vol. 91, no. 12, pp. 2043–2067, 2003.

[2] F.-Y. Wang, "Parallel control and management for intelligent transportation systems: Concepts, architectures, and applications," *IEEE Transactions on Intelligent Transportation Systems*, vol. 11, no. 3, pp. 630–638, 2010.

[3] M. Ramezani, J. Haddad, and N. Geroliminis, "Dynamics of heterogeneity in urban networks: aggregated traffic modeling and hierarchical control," *Transportation Research Part B: Methodological*, vol. 74, pp. 1–19, 2015.

[4] C. Diakaki, M. Papageorgiou, and K. Aboudolas, "A multivariable regulator approach to traffic-responsive network-wide signal control," *Control Engineering Practice*, vol. 10, no. 2, pp. 183–195, 2002.

[5] A. Kouvelas, K. Aboudolas, M. Papageorgiou, and E. B. Kosmatopoulos, "A hybrid strategy for real-time traffic signal control of urban road networks," *IEEE Transactions on Intelligent Transportation Systems*, vol. 12, no. 3, pp. 884–894, 2011.

[6] P. Varaiya, "Max pressure control of a network of signalized intersections," *Transportation Research Part C: Emerging Technologies*, vol. 36, pp. 177–195, 2013.

[7] A. Kouvelas, J. Lioris, S. Fayazi, and P. Varaiya, "Maximum pressure controller for stabilizing queues in signalized arterial networks," *Transportation Research Record: Journal of the Transportation Research Board*, no. 2421, pp. 133–141, 2014.

[8] A. A. Zaidi, B. Kulcsar, and H. Wymeersch, "Traffic-adaptive signal control and vehicle routing using a decentralized back-pressure method," in *European Control Conference*. IEEE, 2015, pp. 3029–3034.

[9] M. Smith and R. Mounce, "A splitting rate model of traffic re-routeing and traffic control," *Transportation Research Part B: Methodological*, vol. 45, no. 9, pp. 1389–1409, 2011.

[10] M. Smith, "Traffic signal control and route choice: A new assignment and control model which designs signal timings," *Transportation Research Part C: Emerging Technologies*, vol. 58, pp. 451–473, 2015.

[11] J. Godfrey, "The mechanism of a road network," *Traffic Engineering and Control*, vol. 11, no. 7, pp. 323–327, 1969.

[12] N. Geroliminis and C. F. Daganzo, "Existence of urban-scale macroscopic fundamental diagrams: Some experimental findings," *Transportation Research Part B: Methodological*, vol. 42, no. 9, pp. 759–770, 2008.

[13] V. V. Gayah and C. F. Daganzo, "Clockwise hysteresis loops in the macroscopic fundamental diagram: an effect of network instability," *Transportation Research Part B: Methodological*, vol. 45, no. 4, pp. 643–655, 2011.

[14] N. Geroliminis and J. Sun, "Properties of a well-defined macroscopic fundamental diagram for urban traffic," *Transportation Research Part B: Methodological*, vol. 45, no. 3, pp. 605–617, 2011.

[15] V. Knoop, S. Hoogendoorn, and J. Van Lint, "Routing strategies based on macroscopic fundamental diagram," *Transportation Research Record: Journal of the Transportation Research Board*, no. 2315, pp. 1–10, 2012.

[16] Y. Ji, J. Luo, and N. Geroliminis, "Empirical observations of congestion propagation and dynamic partitioning with probe data for large-scale systems," *Transportation Research Record: Journal of the Transportation Research Board*, no. 2422, pp. 1–11, 2014.

[17] M. Saeedmanesh and N. Geroliminis, "Clustering of heterogeneous networks with directional flows based on snake similarities," *Transportation Research Part B: Methodological*, vol. 91, pp. 250–269, 2016.

[18] C. F. Daganzo, "Urban gridlock: Macroscopic modeling and mitigation approaches," *Transportation Research Part B: Methodological*, vol. 41, no. 1, pp. 49–62, 2007.

[19] M. Keyvan-Ekbatani, A. Kouvelas, I. Papamichail, and M. Papageorgiou, "Exploiting the fundamental diagram of urban networks for feedback-based gating," *Transportation Research Part B: Methodological*, vol. 46, no. 10, pp. 1393–1403, 2012.

[20] V. V. Gayah, X. S. Gao, and A. S. Nagle, "On the impacts of locally adaptive signal control on urban network stability and the macroscopic fundamental diagram," *Transportation Research Part B: Methodological*, vol. 70, pp. 255–268, 2014.

[21] J. Haddad and A. Shraiber, "Robust perimeter control design for an urban region," *Transportation Research Part B: Methodological*, vol. 68, pp. 315–332, 2014.

[22] J. Haddad, "Optimal coupled and decoupled perimeter control in one-region cities," *Control Engineering Practice*, vol. 61, pp. 134–148, 2017.

[23] J. Haddad and N. Geroliminis, "On the stability of traffic perimeter control in two-region urban cities," *Transportation Research Part B: Methodological*, vol. 46, no. 9, pp. 1159–1176, 2012.

[24] K. Aboudolas and N. Geroliminis, "Perimeter and boundary flow control in multi-reservoir heterogeneous networks," *Transportation Research Part B: Methodological*, vol. 55, pp. 265–281, 2013.

[25] A. Kouvelas, M. Saeedmanesh, and N. Geroliminis, "Enhancing model-based feedback perimeter control with data-driven online adaptive optimization," *Transportation Research Part B: Methodological*, vol. 96, pp. 26–45, 2017.
[26] J. Haddad, "Optimal perimeter control synthesis for two urban regions with aggregate boundary queue dynamics," *Transportation Research Part B: Methodological*, vol. 96, pp. 1–25, 2017.
[27] M. Saberi and H. Mahmassani, "Exploring properties of networkwide flow-density relations in a freeway network," *Transportation Research Record: Journal of the Transportation Research Board*, no. 2315, pp. 153–163, 2012.
[28] M. Yildirimoglu, M. Ramezani, and N. Geroliminis, "Equilibrium analysis and route guidance in large-scale networks with MFD dynamics," *Transportation Research Part C: Emerging Technologies*, vol. 59, pp. 404–420, 2015.
[29] C. E. Garcia, D. M. Prett, and M. Morari, "Model predictive control: theory and practice – a survey," *Automatica*, vol. 25, no. 3, pp. 335–348, 1989.
[30] D. Q. Mayne, J. B. Rawlings, C. V. Rao, and P. O. Scokaert, "Constrained model predictive control: Stability and optimality," *Automatica*, vol. 36, no. 6, pp. 789–814, 2000.
[31] G. Gomes and R. Horowitz, "Optimal freeway ramp metering using the asymmetric cell transmission model," *Transportation Research Part C: Emerging Technologies*, vol. 14, no. 4, pp. 244–262, 2006.
[32] I. Papamichail, A. Kotsialos, I. Margonis, and M. Papageorgiou, "Coordinated ramp metering for freeway networks–a model-predictive hierarchical control approach," *Transportation Research Part C: Emerging Technologies*, vol. 18, no. 3, pp. 311–331, 2010.
[33] M. Hajiahmadi, G. S. van de Weg, C. M. Tampère, R. Corthout, A. Hegyi, B. De Schutter, and H. Hellendoorn, "Integrated predictive control of freeway networks using the extended link transmission model," *IEEE Transactions on Intelligent Transportation Systems*, vol. 17, no. 1, pp. 65–78, 2016.
[34] A. Hegyi, B. De Schutter, and J. Hellendoorn, "Optimal coordination of variable speed limits to suppress shock waves," *IEEE Transactions on Intelligent Transportation Systems*, vol. 6, no. 1, pp. 102–112, 2005.
[35] J. R. D. Frejo, A. Núñez, B. De Schutter, and E. F. Camacho, "Hybrid model predictive control for freeway traffic using discrete speed limit signals," *Transportation Research Part C: Emerging Technologies*, vol. 46, pp. 309–325, 2014.
[36] A. Hegyi, B. De Schutter, and H. Hellendoorn, "Model predictive control for optimal coordination of ramp metering and variable speed limits," *Transportation Research Part C: Emerging Technologies*, vol. 13, no. 3, pp. 185–209, 2005.
[37] A. Karimi, A. Hegyi, B. De Schutter, H. Hellendoorn, and F. Middelham, "Integration of dynamic route guidance and freeway ramp metering using model predictive control," in *American Control Conference, 2004. Proceedings of the 2004*, vol. 6. IEEE, 2004, pp. 5533–5538.
[38] S. Lin, B. De Schutter, Y. Xi, and H. Hellendoorn, "Fast model predictive control for urban road networks via MILP," *IEEE Transactions on Intelligent Transportation Systems*, vol. 12, no. 3, pp. 846–856, 2011.
[39] Z. Zhou, B. De Schutter, S. Lin, and Y. Xi, "Multi-agent model-based predictive control for large-scale urban traffic networks using a serial scheme," *IET Control Theory & Applications*, vol. 9, no. 3, pp. 475–484, 2015.
[40] M. Van den Berg, A. Hegyi, B. De Schutter, and H. Hellendoorn, "Integrated traffic control for mixed urban and freeway networks: A model predictive control approach," *European Journal of Transport and Infrastructure Research EJTIR, 7 (3)*, 2007.
[41] L. Li, R. R. Negenborn, and B. De Schutter, "Distributed model predictive control for cooperative synchromodal freight transport," *Transportation Research Part E: Logistics and Transportation Review*, 2016.
[42] B. Kersbergen, T. van den Boom, and B. De Schutter, "Distributed model predictive control for railway traffic management," *Transportation Research Part C: Emerging Technologies*, vol. 68, pp. 462–489, 2016.
[43] N. Geroliminis, J. Haddad, and M. Ramezani, "Optimal perimeter control for two urban regions with macroscopic fundamental diagrams: A model predictive approach," *IEEE Transactions on Intelligent Transportation Systems*, vol. 14, no. 1, pp. 348–359, 2013.
[44] J. Haddad, M. Ramezani, and N. Geroliminis, "Cooperative traffic control of a mixed network with two urban regions and a freeway," *Transportation Research Part B: Methodological*, vol. 54, pp. 17–36, 2013.
[45] M. Hajiahmadi, J. Haddad, B. De Schutter, and N. Geroliminis, "Optimal hybrid perimeter and switching plans control for urban traffic networks," *IEEE Transactions on Control Systems Technology*, vol. 23, no. 2, pp. 464–478, 2015.
[46] M. Hajiahmadi, V. L. Knoop, B. De Schutter, and H. Hellendoorn, "Optimal dynamic route guidance: A model predictive approach using the macroscopic fundamental diagram," in *16th International IEEE Conference on Intelligent Transportation Systems*. IEEE, 2013, pp. 1022–1028.
[47] R. Lamotte and N. Geroliminis, "The morning commute in urban areas: Insights from theory and simulation," in *Transportation Research Board 95th Annual Meeting*, no. 16-2003, 2016.
[48] L. Ambühl and M. Menendez, "Data fusion algorithm for macroscopic fundamental diagram estimation," *Transportation Research Part C: Emerging Technologies*, vol. 71, pp. 184–197, 2016.
[49] M. Diehl, H. J. Ferreau, and N. Haverbeke, "Efficient numerical methods for nonlinear MPC and moving horizon estimation," in *Nonlinear model predictive control*. Springer, 2009, pp. 391–417.
[50] M. Diehl, H. G. Bock, H. Diedam, and P.-B. Wieber, "Fast direct multiple shooting algorithms for optimal robot control," in *Fast motions in biomechanics and robotics*. Springer, 2006, pp. 65–93.
[51] H. G. Bock and K.-J. Plitt, "A multiple shooting algorithm for direct solution of optimal control problems," in *Proceedings of the IFAC World Congress*, 1984.
[52] A. Wächter and L. T. Biegler, "On the implementation of an interior-point filter line-search algorithm for large-scale nonlinear programming," *Mathematical Programming*, vol. 106, no. 1, pp. 25–57, 2006.
[53] J. Andersson, "A General-Purpose Software Framework for Dynamic Optimization," PhD thesis, Arenberg Doctoral School, KU Leuven, Department of Electrical Engineering (ESAT/SCD) and Optimization in Engineering Center, Kasteelpark Arenberg 10, 3001-Heverlee, Belgium, October 2013.
[54] M. Ben-Akiva and M. Bierlaire, "Discrete choice methods and their applications to short term travel decisions," in *Handbook of Transportation Science*. Springer, 1999, pp. 5–33.
[55] M. Keyvan-Ekbatani, M. Yildirimoglu, N. Geroliminis, and M. Papageorgiou, "Multiple concentric gating traffic control in large-scale urban networks," *IEEE Transactions on Intelligent Transportation Systems*, vol. 16, no. 4, pp. 2141–2154, 2015.

Isik Ilber Sirmatel received the B.Sc. degrees in mechanical and control engineering from Istanbul Technical University, Turkey, and the M.Sc. degree in mechanical engineering from Swiss Federal Institute of Technology in Zurich, Switzerland, in 2010, 2012, and 2014, respectively. He is currently working toward the Ph.D. degree in electrical engineering at the Urban Transport Systems Laboratory (LUTS), School of Architecture, Civil and Environmental Engineering, Swiss Federal Institute of Technology in Lausanne (EPFL), Switzerland. His research interests include automatic control, optimization, and model predictive control, with applications to control of transportation systems.

Nikolas Geroliminis is an Associate Professor at EPFL and the head of the Urban Transport Systems Laboratory (LUTS). Before joining EPFL he was an Assistant Professor on the faculty of the Department of Civil Engineering at the University of Minnesota. He has a diploma in Civil Engineering from the National Technical University of Athens (NTUA) and an M.Sc. and Ph.D. in civil engineering from University of California, Berkeley. He is a member of the Transportation Research Board's Traffic Flow Theory Committee. He also serves as an Associate Editor in Transportation Research, part C, Transportation Science and IEEE Transactions on ITS and in the editorial board of Transportation Research, part B, Journal of ITS and of many international conferences. His research interests focus primarily on urban transportation systems, traffic flow theory and control, public transportation and logistics, on-demand transportation, optimization and large scale networks. He is a recent recipient of the ERC starting grant "METAFERW: Modeling and controlling traffic congestion and propagation in large-scale urban multimodal networks".